HHS Public Access

Author manuscript

Cell Rep. Author manuscript; available in PMC 2017 September 19.

Published in final edited form as:

Cell Rep. 2017 March 28; 18(13): 3143–3154. doi:10.1016/j.celrep.2017.03.010.

Enhanced degradation of misfolded proteins promotes tumorigenesis

Liang Chen[1], **Michael D. Brewer**[1,2], **Lili Guo**[1], **Ruoxing Wang**[1], **Peng Jiang**[1,3], and **Xiaolu Yang**[1,*]

[1]Department of Cancer Biology and Abramson Family Cancer Research Institute, Perelman School of Medicine, University of Pennsylvania, Philadelphia, PA 19104, USA

SUMMARY

An adequate cellular capacity to degrade misfolded proteins is critical for cell survival and organismal health. A diminished capacity is associated with aging and neurodegenerative diseases; however, the consequences of an enhanced capacity remain undefined. Here we report that the ability to clear misfolded proteins is increased during oncogenic transformation, and is reduced upon tumor cell differentiation. The augmented capacity mitigates oxidative stress associated with oncogenic growth, and is required for both the initiation and maintenance of malignant phenotypes. We show that tripartite motif-containing (TRIM) proteins select misfolded proteins for proteasomal degradation. The higher degradation power in tumor cells is attributed to the up-regulation of proteasome activity and especially TRIM proteins, both mediated by the anti-oxidant transcription factor Nrf2. These findings establish a critical role of TRIMs in protein quality control, connect the clearance of misfolded proteins to anti-oxidant defense, and suggest an intrinsic characteristic of tumor cells.

Keywords

Misfolded proteins; oncogenic transformation; proteasome; TRIM proteins; ROS; anti-oxidant defense; Nrf2; TRIM11; breast cancer; PML

INTRODUCTION

Proteins, which account for approximately 50% of the dry mass of the cell, face constant challenges in folding into and maintaining their native conformations (Balch et al., 2008). To contend with protein misfolding, cells employ two major classes of protein quality control (PQC) systems: (1) chaperone systems, consisting of various stress-induced heat shock proteins (HSPs) and their constitutively expressed relatives, that facilitate correct protein folding, and (2) degradation systems, including autophagy and especially the ubiquitin-

*Correspondence: xyang@mail.med.upenn.edu.
[2]Current address: Food and Drug Administration, 7500 Standish Place, Rockville, MD 20855
[3]Current Address: School of Life Sciences, Tsinghua University, Beijing, China, 100084.
Leading Contact: Xiaolu Yang

AUTHOR CONTRIBUTIONS

L.C. and X.Y. designed the study, analyzed the data, and wrote the manuscript. L.C. conducted the great majority of experiments. M.D.B., L.G., R.W., and P.J. conducted experiments.

proteasome system (UPS), that recycle aberrantly folded proteins (Kim et al., 2013; Tyedmers et al., 2010). Since protein misfolding is inevitable and often cannot be reversed, degradation systems likely afford cells the ultimate defense against protein misfolding (Goldberg, 2003; Tyedmers et al., 2010).

The accumulation of misfolded proteins is associated with aging and a multitude of debilitating diseases including neurodegenerative disorders (e.g. Alzheimer's disease), nonneuropathic systemic amyloidosis, and type II diabetes (Labbadia and Morimoto, 2015). Therefore, an insufficient PQC capacity is generally considered to be undesirable for cellular function and organismal health. In contrast, the consequences of a significantly enhanced PQC capacity are poorly defined. Molecular chaperones and their regulators have been implicated in tumorigenesis. Of note, heat shock factor 1 (HSF1), a master regulator of cellular response to protein-damaging stresses, is constitutively active in various tumor cells, stimulating the expression of a myriad of genes involved in cell survival and proliferation (Dai et al., 2007; Mendillo et al., 2012). HSP90 facilitates conformational maturation of various mutated or overexpressed oncoproteins such as Akt, Raf-1, and mutant p53 (Calderwood and Gong, 2016). However, given their pleiotropic functions or specific effects on oncoproteins, it remains unclear whether HSF1 and HSP90 promote tumorigenesis by enhancing global protein folding *per se*.

The role of degradation systems in tumorigenesis is even less characterized. A recent study suggested that cancer cells might be under substantial proteotoxic stresses, implying that their capacity to remove misfolded proteins is compromised rather than enhanced (Tang et al., 2015). Our ability to address this issue is hindered by the limited knowledge of how misfolded proteins are selected for degradation. Recently, we identified a role for the tripartite motif-containing (TRIM) protein PML in degrading a variety of misfolded proteins in the nucleus of mammalian cells (Guo et al., 2014). Here we investigate whether the clearance of misfolded proteins is enhanced in tumor cells and, if so, how it may afford an advantage to tumor cell, and what the underlying mechanism may be.

RESULTS

Increased capacity to degrade misfolded proteins during oncogenic transformation

To investigate whether the capacity to degrade misfolded protein is changed during oncogenic transformation, we used a genetically defined model in which primary human mammary epithelial cells (HMECs) are immortalized by the simian virus 40 large T antigen (LT) and the human telomerase catalytic subunit (hTERT), and are then transformed by the oncogene H-Ras^{V12} (Elenbaas et al., 2001) (Figures 1A and 1B). We observed that, compared to HMECs, the immortalized (PHMLEB) and the transformed (PHMLER) cells contained noticeably fewer aggresomes (Figure 1C; Figures S1A–S1C), which are inclusion bodies that harbor misfolded proteins (Johnston et al., 1998), and less insoluble proteins modified by Lys48-linked polyubiquitin chains (K48 polyUb) (Figure 1D), which target proteins for proteasomal degradation. We also examined aberrant, newly synthesized proteins (defective ribosome products or DRiPs), which can account for upwards of 30% of newly synthesized proteins (Schubert et al., 2000). PHMLER cells cleared DRiPs more efficiently than HMECs, as shown by a pulse-chase analysis (Figure 1E; Figure S1D).

To corroborate these observations, we used an exogenous misfolded protein, Atxn1 82Q, a pathogenic ataxin 1 protein with an expanded polyglutamine (polyQ) region (Figure S1E). Atxn1 82Q forms inclusions in the nucleus (Guo et al., 2014) (Figure S1F) and causes spinocerebellar ataxias type 1 (SCA1), a progressive and fatal neurodegenerative disorder (Orr and Zoghbi, 2007). In HMECs, Atxn1 82Q was accumulated to high levels and generated large inclusions; however, it was expressed at low levels and formed small aggregates in PHLEMB and especially in PHMLER cells (Figures 1F and 1G). The Atxn1 82Q mRNA levels were not altered in these cells (Figure S1G). Instead, Atxn1 82Q protein was degraded much faster in PHMLER cells compared to HMECs, as shown by both a cycloheximide (CHX) chase (Figure 1H) and a pulse-chase (Figure 1I) assays. These results indicate that the ability to degrade misfolded proteins is significantly enhanced during HMEC transformation.

Next we evaluated the capacity to degrade misfolded proteins in human breast cancer cell lines. Compared to the normal human mammary epithelial MCF 10A cells, breast cancer MCF7 and MDA-MB-231 cells contained substantially less insoluble K48 polyUb-modified proteins (Figure 1J), and removed DRiPs at a faster rate (Figure 1K; Figure S1H). Also, Atxn1 82Q was accumulated to much lower levels in MCF7, MDA-MB-231, and another breast cancer cell line (SKBR3) compared to MCF 10A (Figure 1L and S1I), due to an accelerated degradation rate (Figure 1M; Figure S1J).

To extend these analyses, we employed a structurally destabilized mutant of the model chaperone substrate *firefly* luciferase (FlucDM) (Gupta et al., 2011), in both the nucleus- and cytoplasm-localized forms. Nuclear FlucDM protein was highly stable in MCF 10A cells (half-life >12 h); however, it was unstable in the initial three, as well as an additional five (T47D, Hs 578T, MDA-MB-436, MDA-MB-468, and MDA-MB-157), human breast cancer cell lines (half-life ~3 to 6 h) (Figures S1K and S1L). Likewise, cytoplasmic FlucDM protein was stable in MCF 10A cells, but was highly unstable in breast cancer cells (Figure S1K). The degradation of FlucDM proteins in breast cancer cells was abrogated by the proteasome inhibitor MG132 (Figures S1K and S1L). Thus, breast cancer cells are highly effective in degrading misfolded proteins in both nucleus and cytoplasm *via* the proteasome.

Reduced capacity to degrade misfolded proteins upon tumor differentiation

To evaluate the change in degradation capacity during the differentiation of cancer cells, we used acute promyelocytic leukemia (APL), a notable example of differentiation therapy. The vast majority of APLs are associated with the t(15;17) chromosomal translocation, generating a fusion protein of PML and retinoic acid receptor α (RARα) that blocks myeloid differentiation. Treatment with all-trans retinoic acid (ATRA) leads to the degradation of PML-RARα and the differentiation of the immature leukemia cells to mature granulocytes (de The and Chen, 2010) (Figures 1N and 1O). Of note, ATRA-treated APL NB4 cells contained noticeably more aggresomes (~3-fold) (Figure 1P) and accumulated Atxn1 82Q to much higher levels (Figures 1Q and 1R), compared to untreated cells. This was due to a significantly reduced degradation rate of the Atxn1 82Q protein (Figure 1S), rather than an increased expression (Figure S1M). The reduced degradation power was specific for Atxn1 82Q protein, because the nonpathogenic counterpart, Atxn1 30Q (Guo et

al., 2014) (Figure S1E), as well as green fluorescent protein (GFP), was accumulated to similar levels in ATRA-treated and -untreated NB4 cells (Figures S1N and S1O). And it was due to NB4 differentiation rather than ATRA treatment *per se*, because ATRA did not alter the levels of aggresomes in a t(15:17)-negative promyelocytic cell line (HL60) (Figure S1P). Thus, the ability to clear misfolded proteins is markedly reduced upon the differentiation of APL cells to morphologically normal cells.

Accumulation of misfolded proteins inhibits both the initiation and maintenance of malignant phenotypes

To investigate the role of a heightened degradation capacity in tumorigenesis, we forced the accumulation of misfolded proteins in immortalized and malignant cells, to block the outcome of this heightened capacity. When expressed in PHMLEB cells (Figure S3A), Atxn1 82Q (but not Atxn1 30Q) effectively blocked H-Ras^{V12}-mediated transformation, as determined by a soft agar colony formation assay (Figure 2A; Figure S3B). Additionally, we used another pathogenic polyQ protein, Httex1p 97QP, which is associated with Huntington's disease (HD) and is mainly localized to the cytoplasm (Guo et al., 2014; Steffan et al., 2004) (Figure S1E). Httex1p 97QP, but not the nonpathogenic counterpart Httex1p 25QP, also rendered PHMLEB cells highly resistant to H-Ras^{V12}-mediated transformation (Figure 2A; Figures S2A and S2B).

Atxn1 82Q or Httex1p 97QP, but not the wild type polyQ proteins, noticeably impeded anchorage-independent growth of MCF7 cells (Figure 2B; Figure S2C) and PHMLER cells (Figures S2D and S2E). Atxn1 82Q (but not Atxn1 30Q) reduced anchorage-independent growth of NB4 cells, to a level comparable with that of the differentiated counterpart (Figure 2C; Figure S2F). The mutant polyQ proteins, but not the wild type polyQ proteins, also impaired anchorage-independent growth of human colon cancer HCT116 cells (Figure 2D; Figures S2G and S2H).

To evaluate the effect of misfolded proteins on tumorigenicity, we implanted HCT116 cells expressing different polyQ proteins into immunodeficient mice. HCT116 expressing the mutant polyQ proteins generated substantially smaller tumors compared to those expressing the wild type counterparts (Figures 2E–2G). However, despite their strong inhibition on oncogenic growth (i.e. growth in soft agar and in animals), mutant polyQ proteins did not impair the proliferation of HCT116 cells on adherent plates (Figure S2I).

We also forced the accumulation of endogenous misfolded proteins using three proteotoxic agents: the proteasome inhibitor MG132, the protein synthesis inhibitor puromycin (Puro), and the autophagy inhibitor chloroquine (CQ). By testing different doses, we identified a low dose for each that did not inhibit proliferation of (Figure 2H; Figures S2J–S2L), or elevate endogenous misfolded proteins in (Figure 2I), HCT116 cells grown on adherent plates. However, at the same low doses, these agents increased aggresomes in HCT116 cells cultured under suspension conditions (Figure 2I), and correlatively inhibited anchorage-independent growth of HCT116 cells (Figure 2J; Figure S2M), indicating that misfolded proteins are highly detrimental to anchorage-independent growth. Taken together, these results demonstrate that both the initiation and the maintenance of malignant phenotypes rely on effective clearance of misfolded proteins.

Enhanced capability to clear misfolded proteins alleviates oxidative stress

Next we investigated how a heightened degradation capacity may promote oncogenic growth. Previous studies showed that, upon detachment from an extracellular matrix, normal epithelial and endothelial cells accumulate high levels of reactive oxygen species (ROS) leading to growth arrest or apoptosis (Li et al., 1999). The oxidative stress is ameliorated in tumor cells for unclear reasons (Schafer et al., 2009). To examine the relationship between the degradation of misfolded protein and the detoxification of ROS, we compared PHMLER cells and HMECs grown under different conditions. On adherent plates, these cells showed similar levels of ROS; however, in suspension, PHMLER cells contained substantially lower ROS compared to HMECs (Figure 3A), correlating with the different amount of misfolded proteins in these cells (Figure 1C). We also isolated HCT116 that had grown in soft agar (i-HCT116; Figure S3A). When grown under the matrix-attached condition, i-HCT116 and parental HCT116 cells contained similar levels of aggresomes and ROS; however, upon matrix detachment, i-HCT116 cells harbored substantially less aggresomes and ROS (Figures 3B and 3C), and showed a noticeably stronger ability to degrade misfolded proteins (Figures S3B and S3C), compared to parental HCT116 cells. Taken together, these results showed a correlation between efficient removal of misfolded proteins and a strong anti-oxidant defense during anchorage-independent, but not anchorage-dependent, growth.

Expression of pathogenic polyQ proteins had no effect on ROS in matrix-attached HCT116 cells, but markedly increased ROS levels in matrix-detached HCT116 cells (Figure 3D). Moreover, the low doses of MG132, Puro, and CQ strongly elicited oxidative stress in matrix-detached, but not matrix-attached, HCT116 cells (Figure 3E), correlating with their effects on aggresomes (Figure 2I). Therefore, accumulation of misfolded proteins engenders a high oxidative stress during anchorage-independent growth.

Next we treated HCT116 cells expressing mutant and wild type polyQ proteins with the ROS scavenger N-acetyl-L-cysteine (NAC). This completely eliminated their difference in ROS levels (Figure 3F) and in anchorage-independent growth (Figure 3G; Figure S3D). We also fed NAC to mice xenografted with HCT116 cells expressing mutant polyQ proteins. This significantly restored the ability of these cells to form tumors (Figures 2E–2G). Thus, the high oxidative stress elicited by misfolded proteins impairs oncogenic growth.

Increase of proteasome activity and autophagy flux in tumor cells

To investigate the mechanisms underlying the heightened degradation capacity in tumor cells, we evaluated proteasome activity. Of note, all three proteasome activities (chymotrypsin-like, caspase-like, and trypsin-like) were significantly enhanced in PHMLER compared to HMEC cells (Figure 4A; Figures S3E–S3G). Proteasome activity was also higher in MCF7 and MDA-MB-231 cells than in MCF 10A cells (Figure 4B; Figure S3H). Conversely, proteasome activity was reduced in ATRA-treated compared to untreated NB4 cells (Figure 4C).

The dominant proteasome holoenzyme consists of a 20S catalytic core particle and the 19S regulatory particle (Finley, 2009). We noticed that mRNA levels of more than half of the 20S subunits, as well as the majority of the 19S subunits, were increased in PHMLER cells

compared to HMECs (Figures S3I and S3J). Consistently, protein levels of the 20S subunits α and β, as well as the 19S subunits PSMD1 and PSMD11, were elevated in PHMLEB and especially PHMLER cells (Figure 4D). In contrast, the 11S proteasome (also known as PA28 and REG) subunits α, β, and γ remained changed (Figure 4D). Therefore, the higher proteasome activity in PHMLER is likely attributed to the coordinated up-regulation of the subunits of the dominant proteasome holoenzyme.

Next we evaluated autophagic activity. Using a GFP fusion of microtubule-associated protein 1 light chain 3 (MAP1LC3; also known as LC3) to mark autophagic membranes (Kaur and Debnath, 2015), we observed that autophagosomes were progressively increased during the transformation of HMECs (Figure 4E; Figure S3K), and were also more numerous in MDA-MB-231 and MCF7 compared with MCF 10A (Figure 4F; Figure S3L). The higher autophagic activity in tumor cells was further demonstrated by increased lipidation of LC3 (LC3-I) with phosphatidylethanolamine (PE) (LC3-II), and by reduced autophagy cargo receptor p62 (Figure 4G). Furthermore, knocking down ATG7 (autophagy-related protein 7) in PHMLER cells led to the accumulation of Atxn1 82Q (Figure 4H).

To assess the relative contributions of the proteasome and autophagy in the removal of misfolded proteins, we used compounds that either block or enhance these two degradation systems. Inhibition of the proteasome by epoxomicin resulted in a higher accumulation of Atxn1 82Q than the blockage of autophagy by CQ (Figure 4I). Activating the proteasome by IU1 (Lee et al., 2010) strongly accelerated the degradation of Atxn1 82Q, while activating autophagy by rapamycin had a moderate effect (Figure 4J; Figure S3M). Therefore, an increase in both the proteasome and autophagic activities likely contributes to the higher degradation capacity in tumor cells, but the proteasome may have a more profound effect.

Role of TRIMs in the degradation of misfolded proteins

The proteasome and autophagy recycle both correctly and aberrantly folded proteins, while the increase in the degradation power in tumor cells appears to be specific to the latter (Figure 1; Figure S1). Therefore, cellular systems that select misfolded proteins for degradation might also be up regulated. These systems are still poorly understood; however, our recent studies revealed that PML mediates the degradation of misfolded proteins in the nucleus of mammalian cells (Guo et al., 2014). PML (also known as TRIM19) is a member of the large TRIM family, which consists of over 70 members in mice and humans (Ozato et al., 2008). We reasoned that other TRIM proteins may also promote the degradation of misfolded proteins, and their activity may be bolstered in tumor cells.

To test this, we analyzed the expression of all TRIM genes in the HMEC transformation model. The expression of more than half of TRIM genes was significantly increased in PHMLER cells compared to HMECs, while the expression of only a few TRIM genes was decreased (Figures S4A–S4D; Table S1). The most highly up-regulated TRIM genes were TRIM5, 8, 22, and 36 (each ~7–10 folds). Silencing each of these four TRIM proteins by small hairpin RNAs (shRNAs) (Figure S4E) impeded the ability of PHMLER cells to degrade Atxn1 82Q, as shown by both a CHX chase and a pulse-chase assays (Figures 5A and 5B); it also elevated steady-state levels of Atxn1 82Q in these cells (Figure S4F). In contrast, silencing TRIM28, which was not up regulated in PHMLER cells (Figure S4B),

had no effect on Atxn1 82Q (Figures S5G and S5H). For comparison, we examined two ubiquitin ligases previously implicated in the degradation of misfolded proteins, CHIP and NEDD4 (Fang et al., 2014; Qian et al., 2006). Their expression was either slightly (CHIP) or moderately (NEDD4) increased in PHMLER cells (Figure S4D). Depleting CHIP did not influence Atxn1 82Q degradation, while depleting NEDD4 had a temperate effect (Figures S4G and S4H).

A surveyed of public databases (cBioPortal and Oncomine) revealed that TRIM genes were amplified in a wide range of human cancers. For example, at least one but often multiple TRIM genes were amplified in nearly 40% of ~1,000 breast invasive carcinomas, with the most frequently amplified being TRIM11 and TRIM17 (co-amplified in ~15%) (TCGA, 2012). However, the mRNA level of TRIM11, but not TRIM17, was significantly elevated in various breast cancer tissues (Figure S4I) (Curtis et al., 2012). TRIM11 was also up regulated in gliomas, lung cancer (Di et al., 2013; Wang et al., 2016), and other tumors (Figure S5). In contrast, TRIM5, 8, 22, and 36 were not commonly amplified in breast cancer or other cancers; neither was NEDD4 (www.cBioPortal.org) (Figure S5). Additionally, silencing TRIM11 impaired Atxn1 82 degradation more severely than silencing TRIM5, 8, 22, or 36 (Figure S4F). Therefore, we proceeded with more detailed analyses of TRIM11.

The expression of the TRIM11 protein was substantially higher in MCF7 and MDA-MB-231 than in MCF 10A cells, and was progressively increased during HMEC transformation (Figure 5C). Depleting TRIM11 markedly impaired the degradation of Atxn1 82Q in MCF7 and MDA-MB-231 cells (Figure 5D; Figures S6A and S6B), as well as PHMLER cells (Figure 5B; Figures S6C–S6E). However, it did not influence the expression of other TRIMs (Figure S6D), indicating a direct role for TRIM11 in protein quality control. An shRNA-resistant form of wild-type TRIM11 reversed the effect of TRIM11 depletion (Figure 5E; Figure S6F), underscoring the specificity of the shRNA. In contrast, a RING-defective mutant (TRIM11 2A), in which two conserved Cys residues in the RING domain (Cys16 and Cys19) were changed to Ala, had no effect (Figure 5E; Figure S6F), suggesting that an intact RING domain is required for the function of TRIM11.

Conversely, forced expression of TRIM11 reduced inclusions formed by Atxn1 82Q (Figure 5F), as well as levels of the Atxn1 82Q protein in different cell lysate fractions, including NP40-soluble (NS), NP-40-resistant but SDS-soluble (SS), and NP-40- and SDS-resistant (SR) (Figures 5G and 5H). Neither knockdown nor over-expression of TRIM11 affected the Atxn1 82Q mRNA (Figure S6G). Instead, TRIM11 interacted with Atxn1 82Q and promoted its ubiquitination (Figures 5I and 5J). TRIM11-mediated degradation of the Atxn1 82Q was inhibited by MG132 (Figures 5F and 5H). Thus, TRIM11 targets misfolded proteins for proteasomal degradation.

TRIM11 is present in both the nucleus and the cytoplasm (Figure S6H). Knocking down TRIM11 resulted in a marked increase in the levels of the cytoplasm-localized Httex1p 97QP (Figures 67I and S6J). Forced expression of TRIM11 reduced Httex1p 97QP inclusions (Figure 5K). It also decreased Httex1p 97QP levels, especially in the SS and SR fractions (Figures S6K and S6L). TRIM11 accelerated the degradation of the Httex1p 97QP

protein (Figure 5L), rather than altering Httex1p 97QP transcription (Figure S6G). TRIM11 also reduced endogenous misfolded proteins, including insoluble K48 polyUb-modified proteins and DRiPs (Figures 5M and 5N; Figure S6M). In contrast, TRIM17 displayed no inhibitory effect on either Atxn1 82Q or Httex1p 97QP (Figure 5G; Figure S6K). Thus, TRIM11 is critically involved in the removal of misfolded proteins, and its up-regulation likely contributes to the enhanced degradation capacity in tumor cells.

We then wondered how the capacity to degrade misfolded proteins might decline upon the differentiation of NB4 cells. Previous studies showed that ATRA induces the degradation of PML-RARα, but not the wild-type PML, which is also present in NB4 cells (de The and Chen, 2010). Interestingly, compared to PML, PML-RARα possessed a significantly stronger ability to clear Atxn1 82Q (Figures S6N and S6O). Thus, PML-RARα is likely a gain-of-function mutation whose disappearance contributes to the reduced degradation power in differentiated APL cells.

TRIM11 promotes tumorigenesis by enhancing clearance of misfolded proteins and anti-oxidant defense

Next we evaluated the role of TRIMs and especially TRIM11 in oncogenic growth. Knocking down each of the four most highly up-regulated TRIM proteins (TRIM5, 8, 22, and 36) in PHMLER cells led to a strong inhibition of anchorage-independent growth (Figure 6A). Knocking down TRIM11 in HCT116 cells led to a similar effect (Figure 6B). Conversely, forced expression of a mCherry fusion of TRIM11, but not mCherry (Figure 6C), almost completely neutralized the inhibitory effect of pathogenic polyQ proteins on anchorage-independent growth (Figure 6D). It also eliminated the inhibitory effect of these proteins on the growth of xenografted tumors, restoring tumorigenicity to levels observed for control cells (Figures 6E–6G). More, TRIM11 reduced ROS levels in cells expressing mutant polyQ proteins (Figure 6H), and ameliorated oxidative stress in matrix-attached and especially matrix-detached cells (Figure 6I). We conclude that TRIM proteins especially TRIM11 promote tumorigenesis by removing misfolded proteins and reducing oxidative stress during oncogenic growth.

To address the role of the proteasome, we treated PHMLEB cells with the proteasome activator IU1. This led to a substantial increase in H-Ras^{V12}-mediated transformation (Figure 6J; Figures S7A and S7B), supporting the notion that a heightened proteasome activity promotes tumorigenesis.

Nrf1 and especially Nrf2 mediate the up-regulation of the proteasome and TRIMs in tumor cells

Nrf1 and Nrf2 are two key regulators of intracellular antioxidant responses, and both regulate proteasome activity (Arlt et al., 2009; Radhakrishnan et al., 2010; Zhang et al., 2014). We observed that Nrf1 was moderately (~50%), while Nrf2 was strongly (~160%), up regulated in PHMLER cells compared to HMECs; however, the levels of FOXO4, a transcription factor implicated in the regulation of the 19S proteasome subunit PSMD11 (Vilchez et al., 2012), remained unchanged (Figure 7A). Silencing Nrf2 reduced the expression of several proteasome subunits (Figures 7B and 7C), while silencing Nrf1 had a

moderate effect (Figure S8C). Also, proteasome activity in PHMLER cells devoid of Nrf2 was reduced to a level lower than that in HMECs (Figure 7D; Figure S7D). Thus, Nrf1 and especially Nrf2 mediate the up-regulation of the proteasome in PHMLER cells.

Of note, knocking down Nrf2 also strongly reduced the levels of TRIM5, 8, 22, and 36 in PHMLER cells (Figure S7E), as well as the levels of TRIM11 in both PHMLER and HCT116 cells (Figure 7E; Figures S7F and S7G), suggesting that Nrf2 is a key transcriptional regulator for TRIMs. PHMLER cells devoid of Nrf2 contained increased number of aggresomes (Figure 7F) and were ineffective in degrading Atxn1 82Q and Httex1p 97QP (Figures 7G and 7H). Knocking down Nrf2 also impaired anchorage-independent growth (Figure 7I), while over-expressing Nrf2 enhanced cell proliferation (Figure S7H). Interestingly, forced expression of TRIM11 substantially restored the ability of Nrf2-depleted cells to degrade Httex1p 97QP (Figure 7H) and to grow in soft agar (Figure 7J). These results suggest that Nrf2 plays a critical role in degrading misfolded proteins and promoting anchorage-independent growth, and that it functions in part through the up-regulation of the proteasome and TRIM proteins.

DISCUSSION

The link between misfolded proteins and tumorigenesis remains poorly understood. Here we show that the capacity to degrade misfolded proteins is augmented during oncogenic transformation, and is conversely reduced upon tumor cell differentiation. The higher degradation power is attributable to the enhanced proteasome and autophagic activities, and especially to the up-regulation of the TRIM system that selects misfolded proteins for degradation, and is critical for oncogenic growth as an integral part of anti-oxidant defense. We suggest that the increased degradation capacity may be a constitutive element of malignancy.

Cells rely on proteins for virtually all of their biological processes. Yet, given the abundance of proteins, their intrinsic susceptibility to misfolding (Dobson, 2003), and the rapid turnover of many of them (Eden et al., 2011), normal cells likely face the constant challenge in maintaining protein quality. Moreover, incipient and established neoplastic cells frequently encounter stress conditions including oncogenic mutations, hostile microenvironments, inflammation, excessive nutrient uptake, and matrix detachment, all of which engender rapid ROS production (Gorrini et al., 2013). Thus, the challenge of removing misfolded proteins is likely to be much greater in these cells. As such, a limited ability to remove misfolded proteins may be a normal constraint for oncogenic transformation that must be overcome by tumor cells.

Functionally, a heightened ability to remove misfolded proteins is critical for anti-oxidant defense. Misfolded proteins in the endoplasmic reticulum can elicit oxidative stress (Haynes et al., 2004). Here we demonstrate that misfolded proteins in the cytoplasm and nucleus enable a similar effect. Given that elevated levels of ROS can damage proteins (and other cellular constituents), oxidative stress and misfolded proteins can form a vicious cycle. We find that misfolded proteins are highly detrimental for oncogenic growth, while having a minimal effect on adherent proliferation. Thus, the high oxidative stress associated with

oncogenic growth likely demands a robust capability to eliminate misfolded proteins, preventing a runaway vicious cycle that can elevate ROS to levels incompatible with tumor formation and maintenance.

Mechanistically, this higher degradation activity is attributable in part to the enhanced expression of the subunits of the predominant proteasome holoenzyme. Increasing proteasome activity can also promote oncogenic transformation. Thus, our findings support the notion that the proteasome can become limiting for tumorigenesis, and adapting proteasome levels might be an integral part of cellular transformation. The enhanced degradation power is also ascribed to the enhanced functions of TRIM proteins, either through transcriptional up-regulation, as in the case of breast cancer cells, or the formation of gain-of-function fusions, as observed in APL cells. Although it has long been recognized that the UPS is critical for degrading misfolded proteins, an outstanding issue is how misfolded proteins, especially those in the cytoplasm and the nucleus of mammalian cells, are specifically recognized and targeted for degradation (Goldberg, 2003; Tyedmers et al., 2010). We previously reported that PML mediates the degradation of misfolded proteins in the nucleus of mammalian cells (Chu and Yang, 2011; Guo et al., 2014). Here we demonstrate that TRIM11 (and likely some other TRIM proteins) share this property, and it operates in both the nucleus and the cytoplasm. Moreover, TRIM11 promotes the degradation of newly synthesized defective proteins, which are likely a major source of misfolded proteins in cells. Given their large number, TRIM proteins likely constitute a major PQC system in metazoan cells.

TRIM-mediated degradation of misfolded proteins effectively mitigates oxidative stresses elicited by misfolded proteins, and restores tumor growth, further underscoring the importance of effectively removing misfolded proteins in the growth and redox balance of tumor cells. Nevertheless, given their diverse functions, it will be interesting to determine whether TRIM proteins may modulate tumorigenesis via additional mechanisms. Of note, TRIM proteins, as well as proteasome subunits, are regulated by Nrf1 and especially Nrf2. Forced expression of TRIM11 can largely rescue the growth defects of tumor cells devoid of Nrf2, indicating a critical role of TRIM proteins, especially TRIM11, in Nrf2-mediated anti-oxidant defense.

Neurodegeneration and cancer manifest in an enigmatic inverse correlation, and patients with polyQ diseases, including SCAs and HD, have a ~50% reduced incidence of most cancers compared to the general population (Ji et al., 2012). Our observations that tumor cells highly rely on an augmented degradation capacity for their growth may provide a plausible explanation. The accumulation of pathogenic polyQ proteins, which are expressed in multiple tissues in affected patients, likely impedes incipient tumor cells from reaching the fully transformed state. Thus, the capability in normal cells to degrade misfolded proteins may be maintained at proper levels, avoiding the adverse effects of excessive misfolded proteins and balancing the need to protect against unscheduled growth. We suggest that the effect of the chaperone systems in tumorigenesis is due in part to an increased folding power for global proteins. Therefore, a robust PQC capacity through the up-regulation of both chaperone and degradation systems may provide a fostering cellular environment for oncogenic transformation. Inhibitors for the molecular chaperones HSP90

are selectively toxic to tumor cells (Trepel et al., 2010). We propose that the inordinate reliance of oncogenic growth on the effective removal of misfolded proteins, and the critical involvement of TRIM proteins in this process, should be exploited for the development of novel therapies.

EXPERIMENTAL PROCEDURES

Aggresome measurements

Aggresomes were analyzed with ProteoStat® aggresome dye (Enzo Life Sciences) according to the manufacture's instruction. See the Supplemental Information for details.

Cell lysate fractionation, western blot, and filter retardation assay

Cell lysates fractionation and filter retardation assay were performed as previously described (Guo et al., 2014). See the Supplemental Information for details.

Pulse-chase assay

Pulse-chase analysis of the degradation of DRiPs (Schubert et al., 2000) and Atxn1 82Q (Guo et al., 2014) were performed as previously described.

ROS measurements

ROS measurements were examined as previously described (Jiang et al., 2013). Briefly, cells were treated with 10 μM H2-DCFDA for 30 min, washed with PBS, and harvested. The DCF signals were immediately measured by a BD Accuri™ C6 flow cytometer (BD Biosciences) and analyzed by FlowJo software.

26S Proteasome Activity Assay

The activity of the 26S proteasome was assayed as previously described (Kisselev and Goldberg, 2005). Cells were lysed, centrifuged and the protein concentrations were measured. Diluted with 26S proteasome assay buffer and incubated with fluorogenic substrates. Proteasome activity was measured by using the substrate Suc-LLVY-AMC, Ac-nLPnLD, and Ac-RLR-AMC (Enzo), respectively. See the Supplemental Material for details.

Tumor xenograft

Cells (2 × 106) were mixed with matrigel membrane (BD Biosciences) and were injected subcutaneously into the flanks of 4–6 week old athymic Balb-c nu/nu male mice (Taconic Farms, Germantown, NY, USA). Tumor length and width were evaluated every 2 days by vernier caliper, and the tumor volume was calculated by the formula $\pi/6\times$ (width) 2 × length. For NAC treatment, mice were fed with drinking water containing 40 mM NAC, which was changed every 3 days. Sixteen days post-injection, mice were euthanized, and solid tumors were removed and weighed. All animal experiments were performed in accordance with relevant guidelines and regulations and were approved by the University of Pennsylvania Institutional Animal Care and Use Committee (IACUC).

Data analysis

All experiments were repeated at least three times. The bands of western blot were quantified using ImageJ (National Institutes of Health). Data analysis was used with GraphPad Prism 5 software (GraphPad Software, USA) through the unpaired two-tailed Student's *t*-test with *p* values denoted as $*p < 0.05$, $**p < 0.01$, and $***p < 0.001$ (n.s, not significant).

See the Supplemental Information for the Supplemental Experimental Procedures and Associated References.

Supplementary Material

Refer to Web version on PubMed Central for supplementary material.

Acknowledgments

We thank W. Prall, G. Zhu, and Y. Zhang for technical assistance; and H. Y. Chang, S. Cherry, A. García-Sastre, M. Lanotte, J. L. Marsh, A. J. Minn, H. T. Orr, S. Raychaudhuri, J. L. Riley, G. L. Semenza, N. Takahashi, B. Vogelstein, and R. A. Weinberg for cell lines and/or plasmids. Supported by grants from the National Institutes of Health (CA088868, CA182675, and CA184867) and a sponsored research agreement from Wealth Strategy Holding Limited to X.Y. M.D.B. was a predoctoral appointee of an NIH training grant (T32-GM-008076). M.D.B. participated in the preparation of this paper in his private capacity. No official support or endorsement by the FDA is intended or should be inferred.

References

Arlt A, Bauer I, Schafmayer C, Tepel J, Muerkoster SS, Brosch M, Roder C, Kalthoff H, Hampe J, Moyer MP, et al. Increased proteasome subunit protein expression and proteasome activity in colon cancer relate to an enhanced activation of nuclear factor E2-related factor 2 (Nrf2). Oncogene. 2009; 28:3983–3996. [PubMed: 19734940]

Balch WE, Morimoto RI, Dillin A, Kelly JW. Adapting proteostasis for disease intervention. Science. 2008; 319:916–919. [PubMed: 18276881]

Calderwood SK, Gong J. Heat shock proteins promote cancer: it's a protection racket. Trends Biochem Sci. 2016; 41:311–323. [PubMed: 26874923]

Chu Y, Yang X. SUMO E3 ligase activity of TRIM proteins. Oncogene. 2011; 30:1108–1116. [PubMed: 20972456]

Curtis C, Shah SP, Chin SF, Turashvili G, Rueda OM, Dunning MJ, Speed D, Lynch AG, Samarajiwa S, Yuan Y, et al. The genomic and transcriptomic architecture of 2,000 breast tumours reveals novel subgroups. Nature. 2012; 486:346–352. [PubMed: 22522925]

Dai C, Whitesell L, Rogers AB, Lindquist S. Heat shock factor 1 is a powerful multifaceted modifier of carcinogenesis. Cell. 2007; 130:1005–1018. [PubMed: 17889646]

de The H, Chen Z. Acute promyelocytic leukaemia: novel insights into the mechanisms of cure. Nat Rev Cancer. 2010; 10:775–783. [PubMed: 20966922]

Di K, Linskey ME, Bota DA. TRIM11 is overexpressed in high-grade gliomas and promotes proliferation, invasion, migration and glial tumor growth. Oncogene. 2013; 32:5038–5047. [PubMed: 23178488]

Dobson CM. Protein folding and misfolding. Nature. 2003; 426:884–890. [PubMed: 14685248]

Eden E, Geva-Zatorsky N, Issaeva I, Cohen A, Dekel E, Danon T, Cohen L, Mayo A, Alon U. Proteome half-life dynamics in living human cells. Science. 2011; 331:764–768. [PubMed: 21233346]

Elenbaas B, Spirio L, Koerner F, Fleming MD, Zimonjic DB, Donaher JL, Popescu NC, Hahn WC, Weinberg RA. Human breast cancer cells generated by oncogenic transformation of primary mammary epithelial cells. Genes Dev. 2001; 15:50–65. [PubMed: 11156605]

Fang NN, Chan GT, Zhu M, Comyn SA, Persaud A, Deshaies RJ, Rotin D, Gsponer J, Mayor T. Rsp5/Nedd4 is the main ubiquitin ligase that targets cytosolic misfolded proteins following heat stress. Nat Cell Biol. 2014; 16:1227–1237. [PubMed: 25344756]

Finley D. Recognition and processing of ubiquitin-protein conjugates by the proteasome. Annu Rev Biochem. 2009; 78:477–513. [PubMed: 19489727]

Goldberg AL. Protein degradation and protection against misfolded or damaged proteins. Nature. 2003; 426:895–899. [PubMed: 14685250]

Gorrini C, Harris IS, Mak TW. Modulation of oxidative stress as an anticancer strategy. Nat Rev Drug Discov. 2013; 12:931–947. [PubMed: 24287781]

Guo L, Giasson BI, Glavis-Bloom A, Brewer MD, Shorter J, Gitler AD, Yang X. A cellular system that degrades misfolded proteins and protects against neurodegeneration. Mol Cell. 2014; 55:15–30. [PubMed: 24882209]

Gupta R, Kasturi P, Bracher A, Loew C, Zheng M, Villella A, Garza D, Hartl FU, Raychaudhuri S. Firefly luciferase mutants as sensors of proteome stress. Nat Methods. 2011; 8:879–884. [PubMed: 21892152]

Haynes CM, Titus EA, Cooper AA. Degradation of misfolded proteins prevents ER-derived oxidative stress and cell death. Mol Cell. 2004; 15:767–776. [PubMed: 15350220]

Ji J, Sundquist K, Sundquist J. Cancer incidence in patients with polyglutamine diseases: a population-based study in Sweden. Lancet Oncol. 2012; 13:642–648. [PubMed: 22503213]

Jiang P, Du W, Mancuso A, Wellen KE, Yang X. Reciprocal regulation of p53 and malic enzymes modulates metabolism and senescence. Nature. 2013; 493:689–693. [PubMed: 23334421]

Johnston JA, Ward CL, Kopito RR. Aggresomes: a cellular response to misfolded proteins. J Cell Biol. 1998; 143:1883–1898. [PubMed: 9864362]

Kaur J, Debnath J. Autophagy at the crossroads of catabolism and anabolism. Nat Rev Mol Cell Biol. 2015; 16:461–472. [PubMed: 26177004]

Kim YE, Hipp MS, Bracher A, Hayer-Hartl M, Hartl FU. Molecular chaperone functions in protein folding and proteostasis. Annu Rev Biochem. 2013; 82:323–355. [PubMed: 23746257]

Kisselev AF, Goldberg AL. Monitoring activity and inhibition of 26S proteasomes with fluorogenic peptide substrates. Methods Enzymol. 2005; 398:364–378. [PubMed: 16275343]

Labbadia J, Morimoto RI. The biology of proteostasis in aging and disease. Annu Rev Biochem. 2015; 84:435–464. [PubMed: 25784053]

Lee BH, Lee MJ, Park S, Oh DC, Elsasser S, Chen PC, Gartner C, Dimova N, Hanna J, Gygi SP, et al. Enhancement of proteasome activity by a small-molecule inhibitor of USP14. Nature. 2010; 467:179–184. [PubMed: 20829789]

Li AE, Ito H, Rovira II, Kim KS, Takeda K, Yu ZY, Ferrans VJ, Finkel T. A role for reactive oxygen species in endothelial cell anoikis. Circ Res. 1999; 85:304–310. [PubMed: 10455058]

Mendillo ML, Santagata S, Koeva M, Bell GW, Hu R, Tamimi RM, Fraenkel E, Ince TA, Whitesell L, Lindquist S. HSF1 drives a transcriptional program distinct from heat shock to support highly malignant human cancers. Cell. 2012; 150:549–562. [PubMed: 22863008]

Orr HT, Zoghbi HY. Trinucleotide repeat disorders. Annu Rev Neurosci. 2007; 30:575–621. [PubMed: 17417937]

Ozato K, Shin DM, Chang TH, Morse HC 3rd. TRIM family proteins and their emerging roles in innate immunity. Nat Rev Immunol. 2008; 8:849–860. [PubMed: 18836477]

Qian SB, McDonough H, Boellmann F, Cyr DM, Patterson C. CHIP-mediated stress recovery by sequential ubiquitination of substrates and Hsp70. Nature. 2006; 440:551–555. [PubMed: 16554822]

Radhakrishnan SK, Lee CS, Young P, Beskow A, Chan JY, Deshaies RJ. Transcription factor Nrf1 mediates the proteasome recovery pathway after proteasome inhibition in mammalian cells. Mol Cell. 2010; 38:17–28. [PubMed: 20385086]

Schafer ZT, Grassian AR, Song L, Jiang Z, Gerhart-Hines Z, Irie HY, Gao S, Puigserver P, Brugge JS. Antioxidant and oncogene rescue of metabolic defects caused by loss of matrix attachment. Nature. 2009; 461:109–113. [PubMed: 19693011]

Schubert U, Anton LC, Gibbs J, Norbury CC, Yewdell JW, Bennink JR. Rapid degradation of a large fraction of newly synthesized proteins by proteasomes. Nature. 2000; 404:770–774. [PubMed: 10783891]

Steffan JS, Agrawal N, Pallos J, Rockabrand E, Trotman LC, Slepko N, Illes K, Lukacsovich T, Zhu YZ, Cattaneo E, et al. SUMO modification of Huntingtin and Huntington's disease pathology. Science. 2004; 304:100–104. [PubMed: 15064418]

Tang Z, Dai S, He Y, Doty RA, Shultz LD, Sampson SB, Dai C. MEK guards proteome stability and inhibits tumor-suppressive amyloidogenesis via HSF1. Cell. 2015; 160:729–744. [PubMed: 25679764]

TCGA. Comprehensive molecular portraits of human breast tumours. Nature. 2012; 490:61–70. [PubMed: 23000897]

Trepel J, Mollapour M, Giaccone G, Neckers L. Targeting the dynamic HSP90 complex in cancer. Nat Rev Cancer. 2010; 10:537–549. [PubMed: 20651736]

Tyedmers J, Mogk A, Bukau B. Cellular strategies for controlling protein aggregation. Nat Rev Mol Cell Biol. 2010; 11:777–788. [PubMed: 20944667]

Vilchez D, Boyer L, Morantte I, Lutz M, Merkwirth C, Joyce D, Spencer B, Page L, Masliah E, Berggren WT, et al. Increased proteasome activity in human embryonic stem cells is regulated by PSMD11. Nature. 2012; 489:304–308. [PubMed: 22972301]

Wang X, Shi W, Shi H, Lu S, Wang K, Sun C, He J, Jin W, Lv X, Zou H, et al. TRIM11 overexpression promotes proliferation, migration and invasion of lung cancer cells. J Exp Clin Cancer Res. 2016; 35:100. [PubMed: 27329103]

Zhang Y, Nicholatos J, Dreier JR, Ricoult SJ, Widenmaier SB, Hotamisligil GS, Kwiatkowski DJ, Manning BD. Coordinated regulation of protein synthesis and degradation by mTORC1. Nature. 2014; 513:440–443. [PubMed: 25043031]

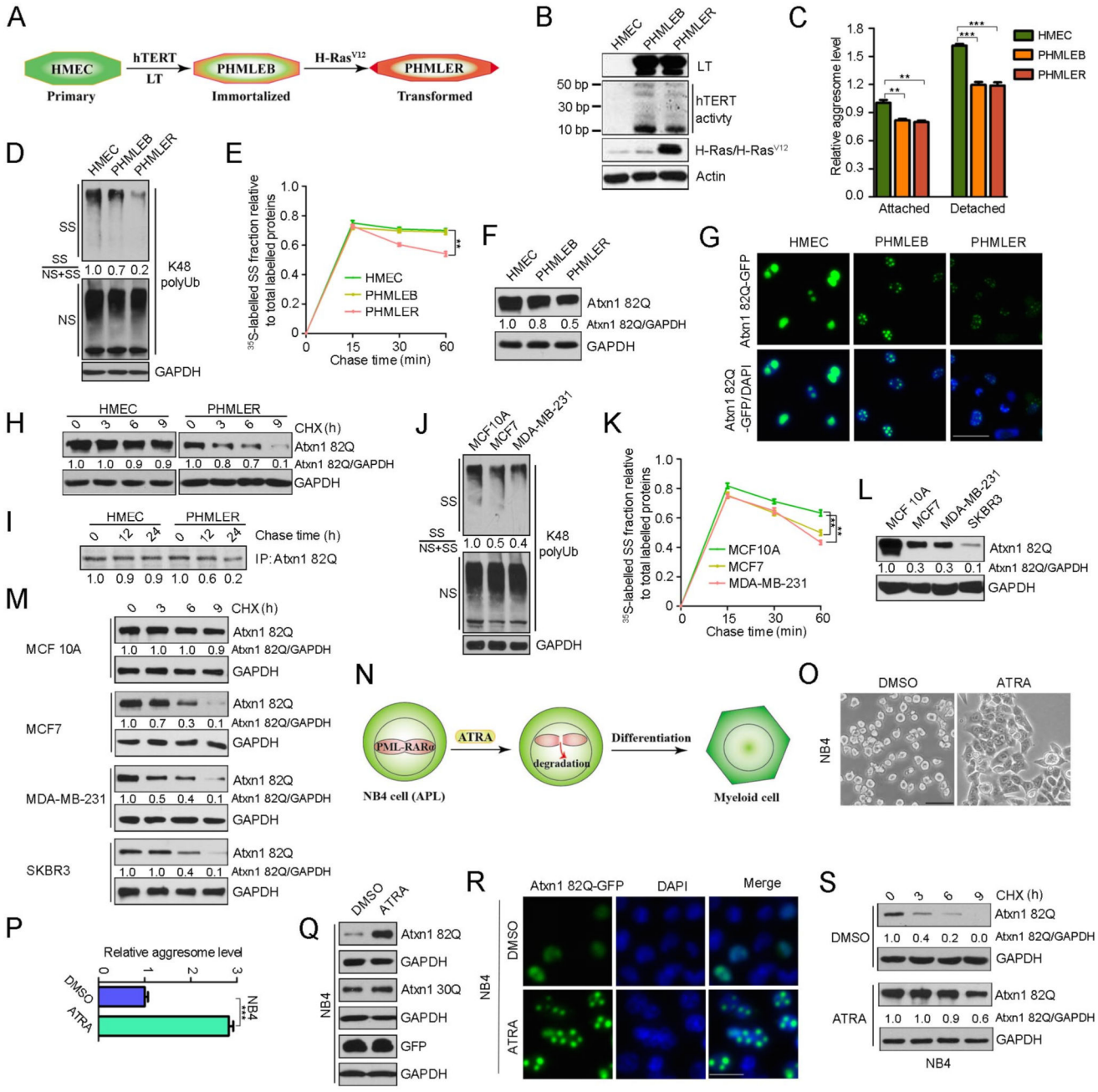

Figure 1. The capacity to clear misfolded proteins is increased during oncogenic transformation and decreased during tumor cell differentiation

(A and B) Schematic diagram of (A), and protein expression/activity in (B), the HMEC transformation model.

(C) Relative levels of aggresomes in matrix-attached and -detached HMEC, PHMLEB, and PHMLER.

(D and J) Reduced K48 polyUb-modified proteins during HMEC transformation (D) and in breast cancer cells (J). NS, NP-40-soluble; SS, NP-40-insoluble and SDS-soluble. Relative ratios of K48 polyUb in the SS versus total (NS + SS) fractions were quantitated based on three independent experiments (n = 3; SD = ±4%).

(E and K) Increased clearance of DRiPs during HMEC transformation (E) and in breast cancer cells (K). Relative ratios of [^{35}S]Met-labeled proteins in the SS (DRiPs) fractions versus total labeled proteins (NS + SS) are shown (n = 3; SD = ±2%). The representative images are shown in Figures S1D and S1H.

(F and L) Levels of Flag-Atxn1 82Q stably expressed in the indicated cells, and relative Atxn1 82Q/GAPDH ratios (n = 3; SD = ±3%).

(G) Representative images of cells stably expressing Atxn1 82Q-GFP (green) and stained with DAPI (blue). Scale bar, 50 μm.

(H and M) Stability of Flag-Atxn1 82Q analyzed by cycloheximide (CHX) chase. Relative Atxn1 82Q/GAPDH ratios are shown (n = 3; SD = ±2%).

(I) Stability of Flag-Atxn1 82Q analyzed by pulse-chase. Atxn1 82Q was immunoprecipitated. Levels of [^{35}S]-labeled Atxn1 82Q relative to time 0 are indicated (n = 3; SD = ±2%).

(N) Schematic diagram of ATRA-induced NB4 differentiation.

(O and P) Morphology of (O; scale bar, 50 μm), and relative levels of aggresomes in (P), NB4 cells treated with vehicle (DMSO) or ATRA (1 μM).

(Q) Levels of GFP-Atxn1 82Q, GFP-Atxn1 30Q, and GFP stably expressed in DMSO- or ATRA-treated NB4 cells.

(R and S) Expression (R) and stability (S) of Atxn1 82Q-GFP expressed in DMSO- and ATRA-treated NB4 cells were examined by fluorescence microscope (R; scale bar, 50 μm) and CHX chase (S), respectively.

In (C), (E), (K) and (P), data represent mean or mean ± SEM (n = 3).

See also Figures S1.

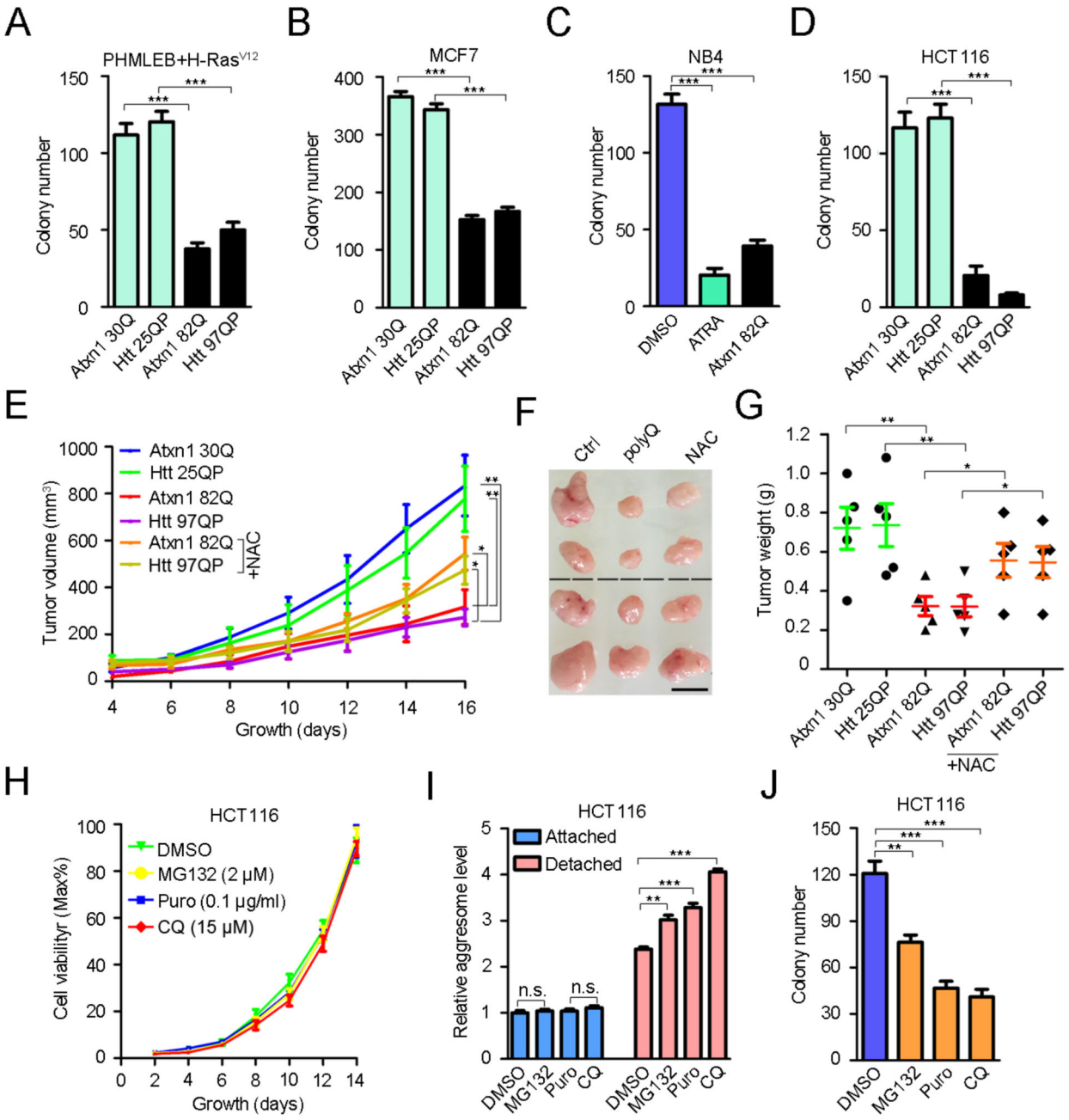

Figure 2. Misfolded proteins impede both the initiation and maintenance of malignant phenotypes

(A) Soft agar colony formation assay of PHMLEB cells stably expressing polyQ proteins and infected with H-Ras^{V12} retroviruses.

(B–D) Soft agar colony formation assay of MCF7 (B), NB4 (C), and HCT116 (D) cells stably expressing polyQ proteins, as well as NB4 cells treated with and without ATRA (C).

(E–G) HCT116 cells expressing polyQ proteins were subcutaneously xenografted into nude mice, which were given water with or without 40 mM NAC. Shown are tumor growths over time (E; n = 5) and representative images (F) and weights (G) of tumors at day 16. In (F), the black dash line separates two independent repeat groups; scale bar, 1 cm.

(H and J) Growth of HCT116 cells on adherent plates (H) and in soft agar (J) in the presence of DMSO (vehicle), MG132 (2 μM), Puro (0.1 μg/ml), or CQ (15 μM).

(I) Aggresomes in matrix-attached and -detached HCT116 cells treated with DMSO, MG132, Puro, or CQ as in (H).

Values are presented as mean (H) or mean ± SEM (the rest) (n = 3).

See also Figure S2.

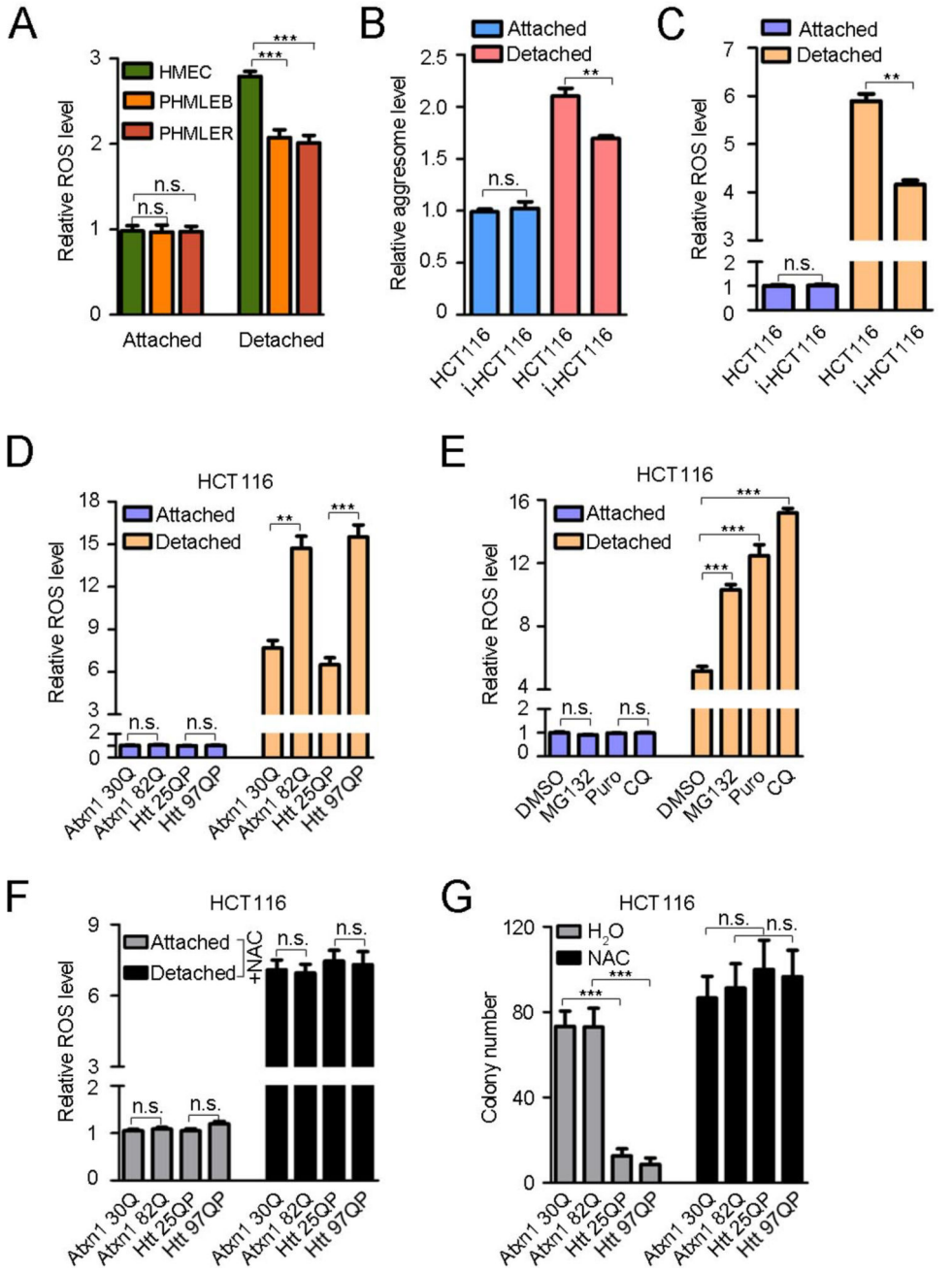

Figure 3. Enhanced capability to clear misfolded proteins alleviates oxidative stress during anchorage-independent growth

(A) Levels of ROS in matrix-attached and -detached HMEC, PHMLEB, and PHMLER.

(B and C) Levels of aggresomes (B) and ROS (C) in matrix-attached and -detached HCT116 and i-HCT116 cells.

(D–F) Levels of ROS in matrix-attached and -detached HCT116 cells expressing polyQ proteins in the absence (D) or presence (F) of 2 mM NAC, or HCT116 cells treated with DMSO, MG132, Puro, or CQ as in Figure 2H (E).

(G) Formation of colonies in soft agar by HCT116 cells expressing polyQ proteins in the absence or presence of 2 mM NAC.

Values are presented as mean ± SEM (n = 3).
See also Figure S3.

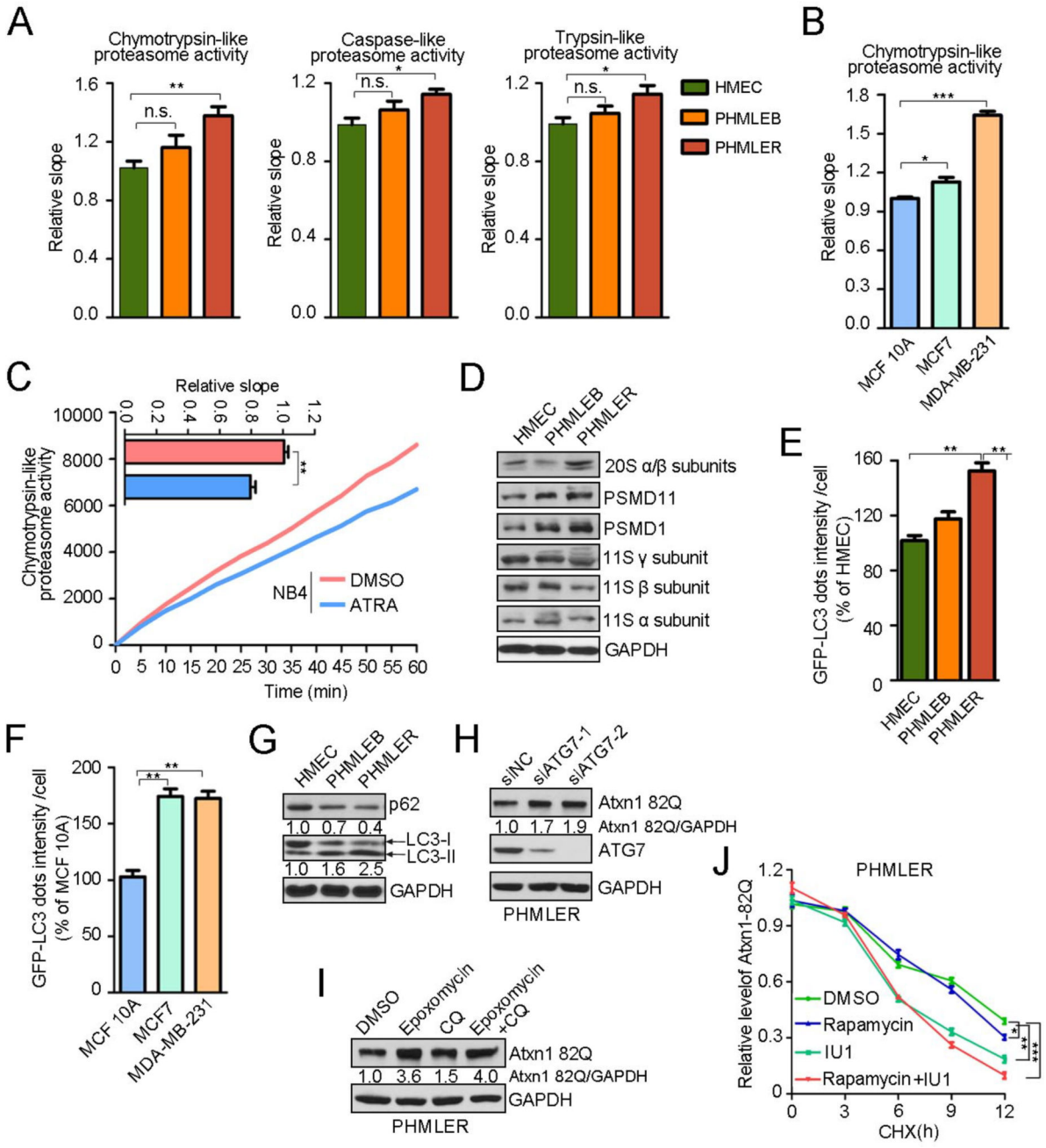

Figure 4. Increase of proteasome and autophagic activities in tumor cells

(A) All three proteasome activities in HMECs, PHLMEB, and PHLMER cells measured by fluorometric substrate (Figures S4E–S4G). Shown are slopes relative to that of HMEC. n = 6 (HMEC), 5 (PHMLEB), or 7 (PHMLER).

(B and C) The chymotrypsin-like proteasome activity in MCF10A, MCF7, and MDA-MB-231 cells (B; Figure S4H), or DMSO- and ATRA-treated NB4 cells (C). n = 7 (MCF 10A), 8 (MCF7, MDA-MB-231, and NB4-DMSO), or 9 (NB4-ATRA).

(D) Levels of 20S proteasome subunits in the HMEC, PHLMEB, and PHLMER.

(E and F) The intensity of GFP-LC3 dots in the indicated cells relative to HMEC (E) or MCF 10A (F), quantified from 300 cells for each sample.
(G) Levels of p62 and LC3 in HMEC, PHLMEB, and PHMLER cells. Relative p62/GAPDH and LC3-II/GAPDH ratios are shown (n = 3; SD = ±3%).
(H) Levels of Atxn1 82Q in PHMLER cells transfected with a control (siNC) and two independent ATG7 siRNAs. Relative ratios of Atxn1 82Q versus GAPDH are indicated (n = 3; SD = ±3%).
(I) Levels of Atxn1 82Q in PHMLER cells treated with DMSO (vehicle), epoxomycin (2 μM), CQ (50 μM), or both epoxomycin and CQ for 8 h. Relative Atxn1 82Q/GAPDH ratios are shown (n = 3; SD = ±3%).
(J) Stability of Atxn1 82Q in PHMLER cells treated with DMSO (vehicle), IU1 (50 μM), rapamycin (100 nM), or both IU1 and rapamycin for 12 h. Relative ratios of Atxn1 82Q and GAPDH were quantified (n = 3).
In (A–C), (E–F) and (J), data represent mean ± SEM (n = 3 unless otherwise indicated). See also Figure S3.

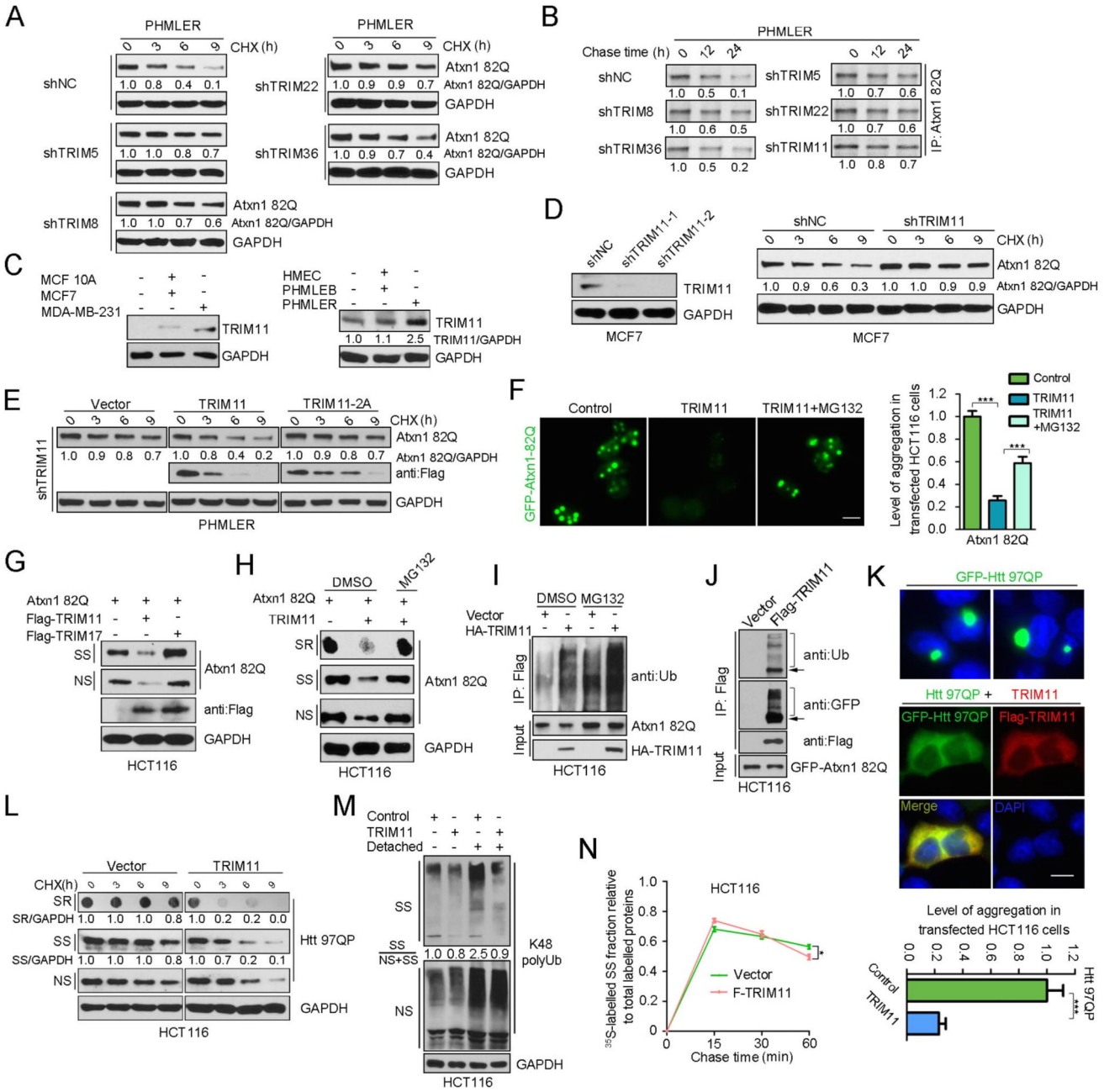

Figure 5. TRIM11 mediates the degradation of misfolded protein in both the nucleus and the cytoplasm

(A and B) Increased stability of Atxn1 82Q in PHMLER cells devoid of TRIM5, 8, 22, or 36, assayed by CHX chase (A) or pulse-chase (B). Relative Atxn1 82Q/GAPDH ratios (A) and levels of [^{35}Met]-labeled Atxn1 82Q (B) are indicated (n =3; SD = ±2%). shNC, control shRNA.

(C) Increased expression of TRIM11 in breast cancer cells (left) and during HMEC transformation (right).

(D) MDA-MB-231 cells stably expressing shNC and TRIM11 shRNAs were analyzed for protein expression (left) and Atxn1 82Q stability (right).

(E) Stability of the Atxn1 82Q in TRIM11-depeleted PHMLER cells infected with control lentiviruses (vector), or lentiviruses expressing shRNA-resistant Flag-TRIM11 or Flag-TRIM11-2A. Relative Atxn1 82Q/GAPDH ratios are indicated (n =3; SD = ±2%).
(F and K) Reduction of Atxn1 82Q and Httex1p 97QP aggregates by TRIM11. HCT116 cells expressing Atxn1 82Q-GFP or Httex1p 97QP-GFP, alone or together with TRIM11, were treated with DMSO or MG132 (F) or untreated (K). Shown are images of GFP fusion proteins in cells (scale bar, 10 μm) and relative numbers of polyQ inclusions (mean ± SEM, n = 3, counted from 200 cells).
(G) Reduction of Atxn1 82Q levels in HCT116 cells by TRIM11, but not TRIM17.
(H) Proteasomal degradation of Atxn1 82Q mediated by TRIM11. Cells transfected with the indicated plasmids and treated with DMSO or MG132 (10 μM) were analyzed by Western blot (NS and SS fractions) and filter retardation assay (for the NP-40- and SDS-resistant or SR fraction).
(I) Ubiquitination of Atxn1 82Q mediated by TRIM11. Flag-Atxn1 82Q-expressing HCT116 cells were transfected with vector or HA-TRIM11, and treated with DMSO or MG132. Extracts containing comparable levels of unmodified Flag-Atxn1 82Q were used for immnoprecipitation with anti-Flag antibody.
(J) GFP-Atxn1 82Q was expressed in HCT116 cells alone or together with Flag-TRIM11. Cell lysates containing comparable amount of Atxn1 82Q were analyzed for the Atxn1 82Q-TRIM11 interaction and Atxn1 82Q ubiquitination. Arrows indicate unmodified Atxn1 82Q.
(L) Acceleration of Httex1p 97QP degradation in HCT116 cells by TRIM11. Relative ratios of Httex1p 97QP/GAPDH are indicated (n =3; SD = ±2%).
(M) K48 polyUb-modified proteins in matrix-attached or -detached HCT116 cells with and without TRIM11 overexpression. Relative ratios of SS versus total (NS+SS) fractions are shown (n = 3; SD = ±4%).
(N) TRIM11 accelerates degradation of DRiPs in HCT116 cells Levels of DRiPs relative to the total [^{35}S]labeled proteins over time are shown (n = 3).
See also Figures S4 and S5.

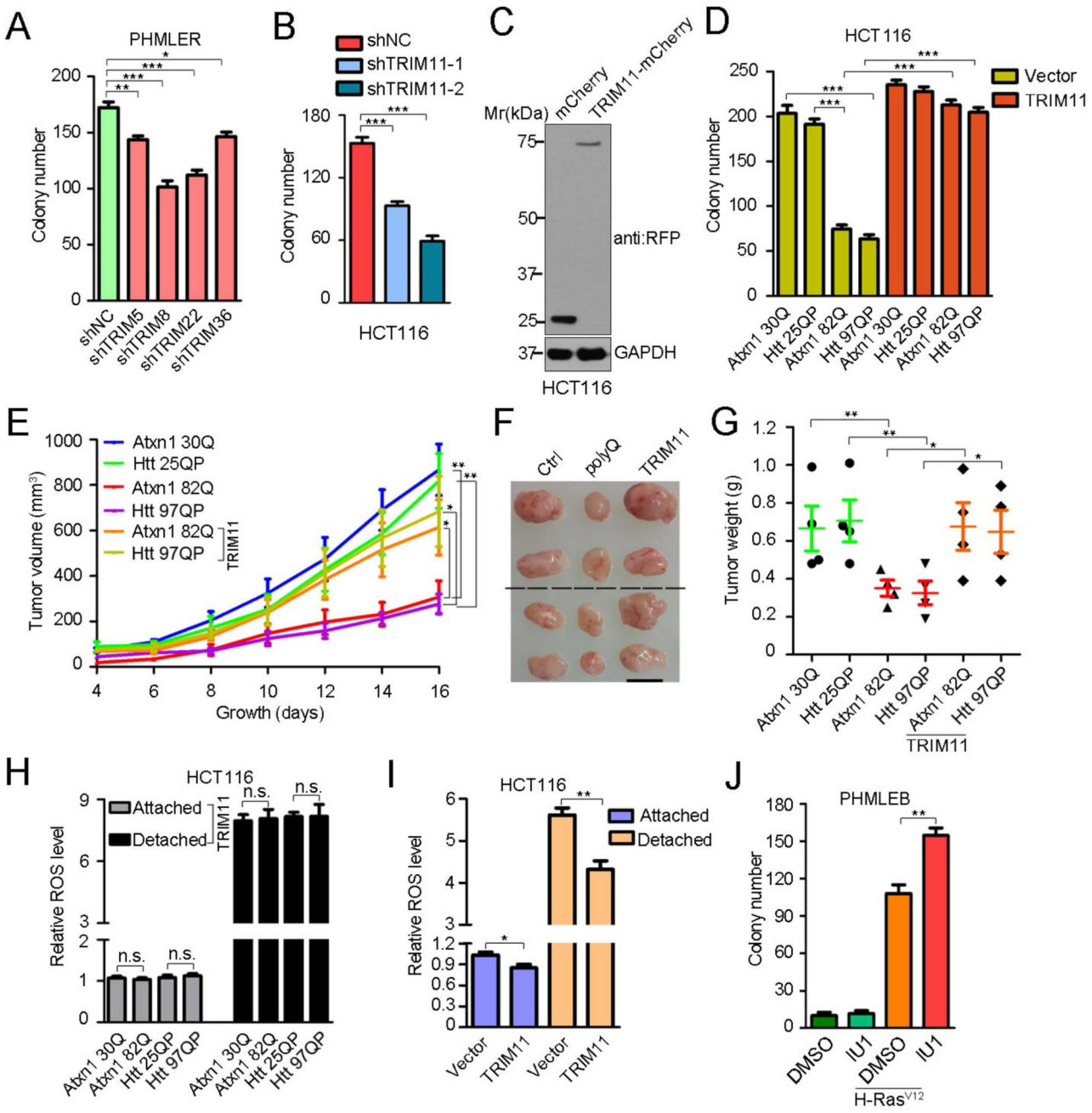

Figure 6. Involvement of TRIM proteins in oncogenic growth

(A, B, and D) Formation of colonies in soft agar by PHMLER or HCT116 cells expressing shNC or the indicated TRIM shRNAs (A and B), or HCT116 cells expressing the indicated polyQ proteins alone or together with TRIM11 (D).

(C) HCT116 cells stably expressing mCherry and TRIM11-mCherry.

(E–G) HCT116 cells expressing the indicated polyQ protein, alone or together with TRIM11, were subcutaneously injected into nude mice. Shown are average tumor volumes over time (n = 4) (E), and representative image (F) and weights (G) of tumors at day 16. In (F), the black dash line separates two independent repeat groups; scale bar, 1 cm.

(H and I) Relative ROS levels in matrix-attached and -detached HCT116 cells (H and I) stably expressing the indicated polyQ proteins and TRIM11 (H), or without and with TRIM11 overexpression (I).

(J) Formation of colonies in soft agar by PHMLEB cells infected with the H-Ras^{V12} retroviruses in the presence of the vehicle (DMSO) or IU1 (50 μM).

All values are presented as mean ± SEM (n = 3 unless otherwise indicated).

See also Figure S6.

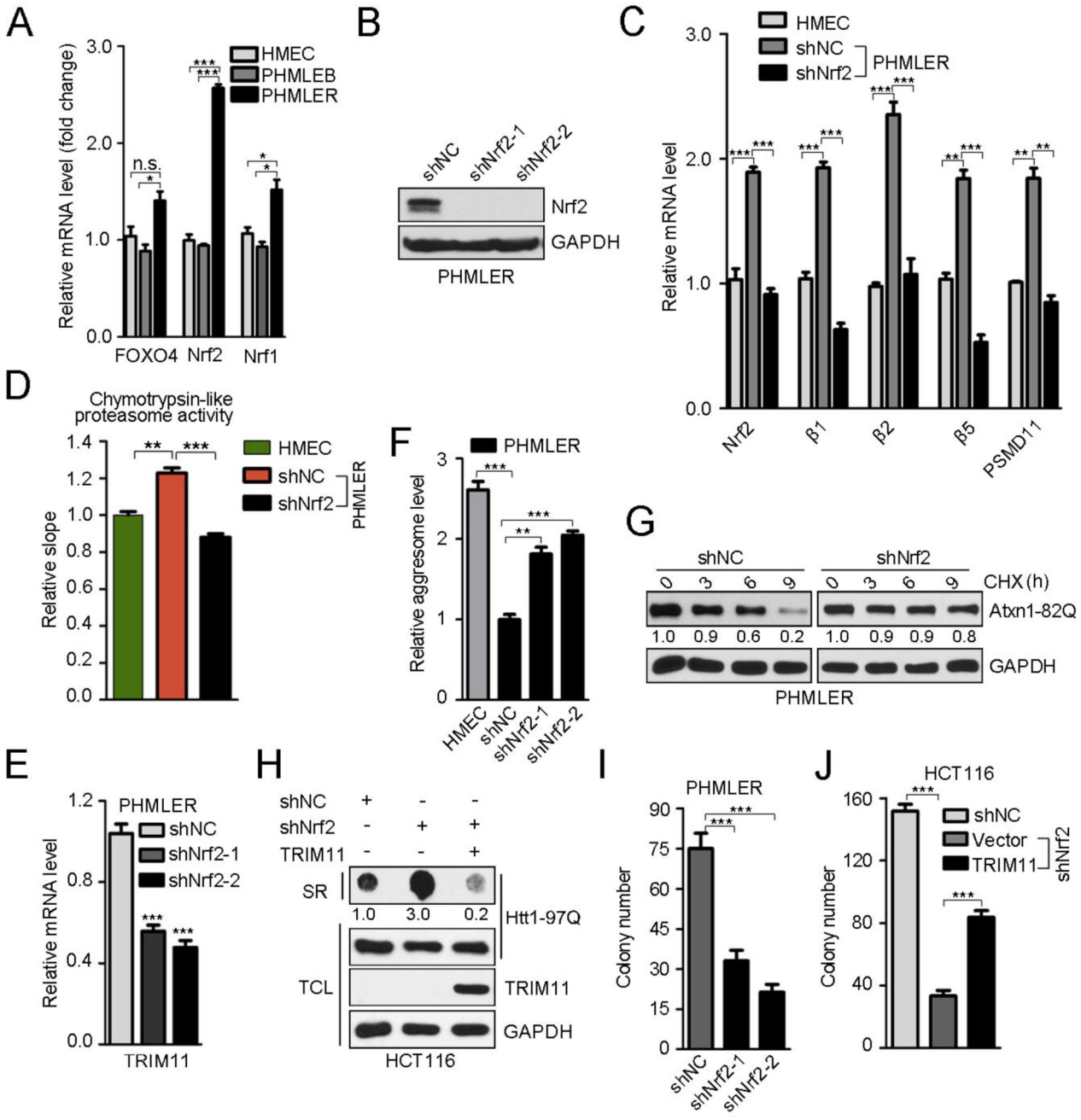

Figure 7. Regulation of TRIMs by Nrf1 and Nrf2, and role of TRIM11 in Nrf2-mediated tumor growth

(A) Relative FOXO4, Nrf1, and Nrf2 mRNA levels during HMEC transformation.

(B–G, and I) shRNA-mediated knockdown of Nrf2 in PMHLER cells (B) and its effect on mRNA levels of proteasome subunits (C), chymotrypsin-like activity of the proteasome (n = 6 or 7) (D), TRIM11 mRNA levels (E), aggresomes (F), the degradation of Atxn1 82Q (for Atxn1 82Q/GAPDH ratios, n = 3, SD = ±2%) (G), and anchorage-independent growth (I).

(H) Httex1p 97QP-expresing HCT116 cells were transfected with shNC, Nrf2 shRNA, and TRIM11 in the indicated combination, and analyzed by Western blot (for total cell lysates,

TCL) or dot blot (for SR fraction). Relative Httex1p 97QP/GAPDH ratios are shown (n = 3, SD = ±2%).

(J) Formation of colonies in soft agar by HCT116 cells stably expressing shNC or Nrf2 shRNA alone, or Nrf2 shRNA plus TRIM11.

Values represent mean ± SEM (n = 3), unless otherwise indicated.

See also Figure S7 and Table S2.